Effect of Axial Pre-Compression on Lateral Performance of Masonry Under Cyclic Loading

SYED HASSAN FAROOQ*, MUHAMMAD ILYAS**, AND ASADULLAH QAZI***

RECEIVED ON 11.03.2009 ACCEPTED ON 13.08.2009

ABSTRACT

Strengthening of masonry against seismic events is very essential and getting maximum attention of researchers around the globe. An extensive experimental program was carried out to study the in-plane lateral performance of un-reinforced masonry, strengthened and retrofitted masonry wall panels under lateral cyclic loading. Twenty tests were carried out; four tests under monotonic lateral loading, twelve tests under static cyclic loading and four tests under pure compression. The test results were analyzed in five groups and this paper presents the analysis of group 4, which deals with effect of axial pre-compression on masonry seismic performance. Three single leaf panels with aspect ratio of 0.67 having size 1.65x1.1m were constructed using same material and workmanship. All the three un-reinforced walls were tested under 0, 0.5 and 1.0MPa vertical pre-compression and displacement controlled static cyclic loading. The wall tested under 0.5MPa pre-compression was reference specimen. The key parameters studied were hysterics behavior, peak lateral load, ultimate lateral displacement, energy dissipation, ductility, response factor and damping ratio. It was observed that level of axial pre-compression has significant effect on lateral capacity, failure mode and performance of masonry. In case of zero pre-compression the lateral capacity was very less and wall went into rocking failure at early stages of loading. Increase in pre-compression to 1.0MPa enhanced the lateral capacity by a factor of 1.92 times. After analysis of test results, it is found that pre-compression has very significant effect on lateral strength, energy dissipation and overall seismic performance.

Key Words: **Masonry Walls, Strengthening Technique, Confinement.**

1. INTRODUCTION

In Pakistan, majority of residential structures, buildings in old parts of cities and monumental buildings are of URM (Un-Reinforced Masonry). Due to aging and lack of maintenance, a large number of the buildings have been declared dangerous. As per Lahore City Government Official record 540 buildings have been declared dangerous out of which 70 buildings are very dangerous and require immediate demolition [1]. Moreover, during 8th October, 2005 earthquake, which struck Northern Areas of Pakistan, a large number of masonry structures were damaged [2-4] and author developed a simple and cost effective technique to combat this problem [5-6]. The main structural element in an URM structure is the wall, which is primarily designed to sustain the gravity loads only and is very vulnerable against seismic events. Under earthquake loading the URM wall can experience in-plane or out-of-

*Ph.D. Scholar, **Professor, and ***Assistant Professor,
Department of Civil Engineering, University of Engineering & Technology, Lahore.

plane forces causing in-plane and out-of-plane failure. The masonry wall under in-plane lateral load can experience diagonal shear cracking, sliding, rocking and toe/heel crushing as shown in Fig. 1. The failure mode of masonry wall mainly depends upon the level of pre-compression, aspect ratio and shear strength of masonry wall panels. It is well-known fact that level of pre-compression has a significant effect on masonry lateral strength and its seismic performance. Almost all the empirical relationships developed by different researchers and given in different codes have catered for the axial load factor in their equations. Matsumura, [7], Shing, et. al. [8], NZS 4230 [9], Anderson, et. al., [10], UBC [11] and Australian Masonry Standard [12] have included the contribution of axial pre-compression towards determination of masonry lateral resistance in their proposed expressions. Matsumura, [13] conducted tests on masonry wall panels to study different parameters and concluded that the lateral resistance of masonry walls increased at a rate of approximately 0.2 times the vertical stress. The lateral capacity of piers in case of shear mode of failure is mainly influenced by the masonry compressive strength, the level of axial pre-compression and aspect ratio with very little influence of vertical steel distribution [14-15]. Woodward [16-17] concluded that the effect of block and mortar strength on shear capacity was almost negligible in case of walls tested under lower levels of axial pre-compressions and it increased with increase in level of axial pre-compression. The lateral cracking load and maximum lateral resistance increased at lower rates with increasing axial load and increase in axial load from 2-26% the increase in shear strength was in the order of 1.6-1.66 times [18]. Kaminosono [19] concluded after the experimentation that increase in axial load and decrease in shear span ratio resulted in increase in lateral capacity with reduction in deformation capacity of masonry walls experiencing shear failure. Shing [20] found that an increase in wall flexural strength was also observed with increase in level of applied axial load but increase in axial load may also cause reduction in ductility capacity. A simple inexpensive effective retrofitting technique is still required. This paper investigates the effect of axial load on in-plane behavior of masonry. The failure mode is very important in performance evaluation of masonry. The in-plane failure mode mainly depends upon the level of pre-compression, aspect ratio, material properties and shear resistance.

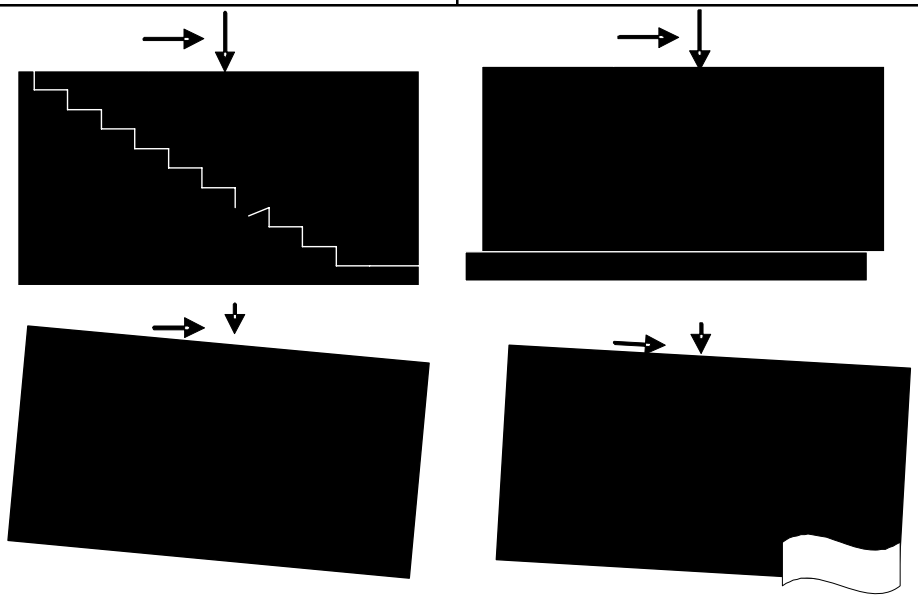

FIG. 1. DIFFERENT FAILURE MODES OF MASONRY; (a) DIAGONAL SHEAR CRACKING, (b) SLIDING, (c) ROCKING, (d) TOE CRUSHING

2. AIM OF RESEARCH

The basic aim and objective of research is to find out the role of axial load on seismic performance of masonry in the local environment. The in-plane cyclic performance of masonry under different level of pre-compression is assessed to establish its effectiveness. The experimental observations and analysis of data for lateral strength; lateral deformation, hysteretic behavior and energy dissipation are the basis for establishing performance of masonry.

3. EXPERIMENTAL PROGRAM AND TEST SET UP

This experimental program investigates the effectiveness of axial pre-compression on in-plane seismic performance of un-reinforced masonry walls. The designation of all the three un-reinforced walls is given in Table 1. Wall-8 was reference wall tested under 0.5Mpa and Wall-6 and Wall-9 were tested under 0 and 1.0Mpa axial pre-compression respectively. Each wall panel rested on RCC foundation beam, which was anchored to the strong floor. RCC cap beam was placed at top of wall panel with the help of S-type mortar for application of lateral and vertical load uniformly. The specimens were tested as cantilever walls and it was fixed at the bottom with the help of bottom anchor and free to move at the top. Manual reversible hydraulic jacks were used to apply lateral load. A combination of vertical compression (representing loads from the building above) and in-plane cyclic lateral load was applied to specimens. A constant vertical pre-compression was applied through connected vertical hydraulic jack. A bridge bearing assembly was used to keep this vertical pre-compression near to constant but still upto 15-20% of variation in vertical load was observed. The lateral cyclic load was applied through hydraulic jacks from both the lateral direction of the wall. The lateral loading was applied at the cap beam, which transferred it to the wall. Both sides of the walls were designated as positive and left side to distinguish the wall behavior in both the direction under cyclic loading. The detailed test set up is shown in Fig. 2 and material properties are summarized in Table 1.

4. TEST SPECIMEN

The test specimens were constructed in the laboratory to represent the typical on going construction practice in Pakistan. Three single wythe walls were constructed using clay brick masonry units with dimension of 228x 115x 76mm. The effective moment/shear ratio was 0.67 with dimensions of 1.6x1.1m. The test specimens were constructed on a concrete filled steel U-channels as shown in Fig. 2 and placed on the bottom anchor beam. All the specimens were cured for 28 days and tested.

5. LOADING HISTORY AND INSTRUMENTATION

LVDTs were used for measuring the lateral displacement; load cells and LVDTs were also used at strain mode for measuring strain in masonry as shown in Fig. 3. Strain Smart 5000 data acquisition system was used to record all data and during testing sixteen channels were utilized. In all the tests, the loading was applied under displacement control to allow monitoring of the complete load deformation response. Keeping in view very less elastic displacement the initial increments were kept as 0.25mm and later rate of increase was kept as 1mm per cycle. The complete loading history is shown in Fig. 4.

TABLE 1. MORTAR CUBE AND MASONRY PRISM TEST RESULTS

Specimen	Wall Designation		Average Compressive Strength (MPa)
Mortar Cubes (ASTM-89 C-109)	Wall 8 (Reference)	URM at 0.5MPa	19.34
	Wall 6	URM at 0MPa	13.98
	Wall 9	URM at 1.0MPa	16.67
Masonry Prisms (ASTM-89 C-1314)	Wall 8	URM at 0.5MPa	9.66
	Wall 6	URM at 0MPa	6.6
	Wall 9	URM at 1.0MPa	8.86

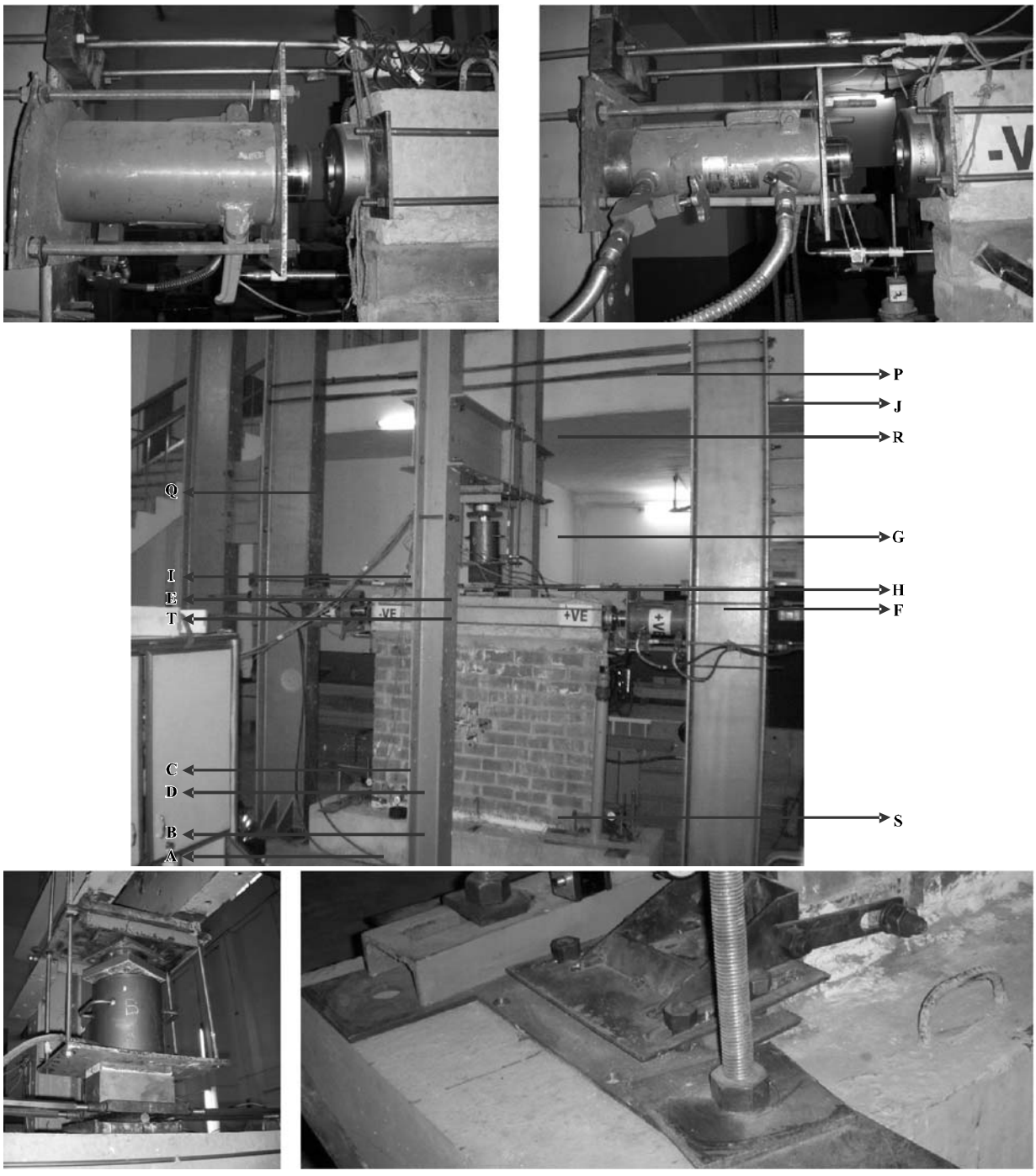

FIG. 2.TEST ARRANGEMENT AND LEGEND

LEGENC:

A Strong Floor
B R.C.C. Foundation Beam
C Anchoring Bolts
D Base lateral anchors
E R.C.C. Cap Beam
F Lateral Load Jack and Load Cell
G Vertical Load Jack and Load Cell
H Bridge Bearing Assembly
Q Frame stiffener
S U-steel channel for lifting
I Horizontal Reaction Anchor Bolts
J Strong Frame
P Top bracing anchors
R Frame for compression load
T Load cell anchor assembly

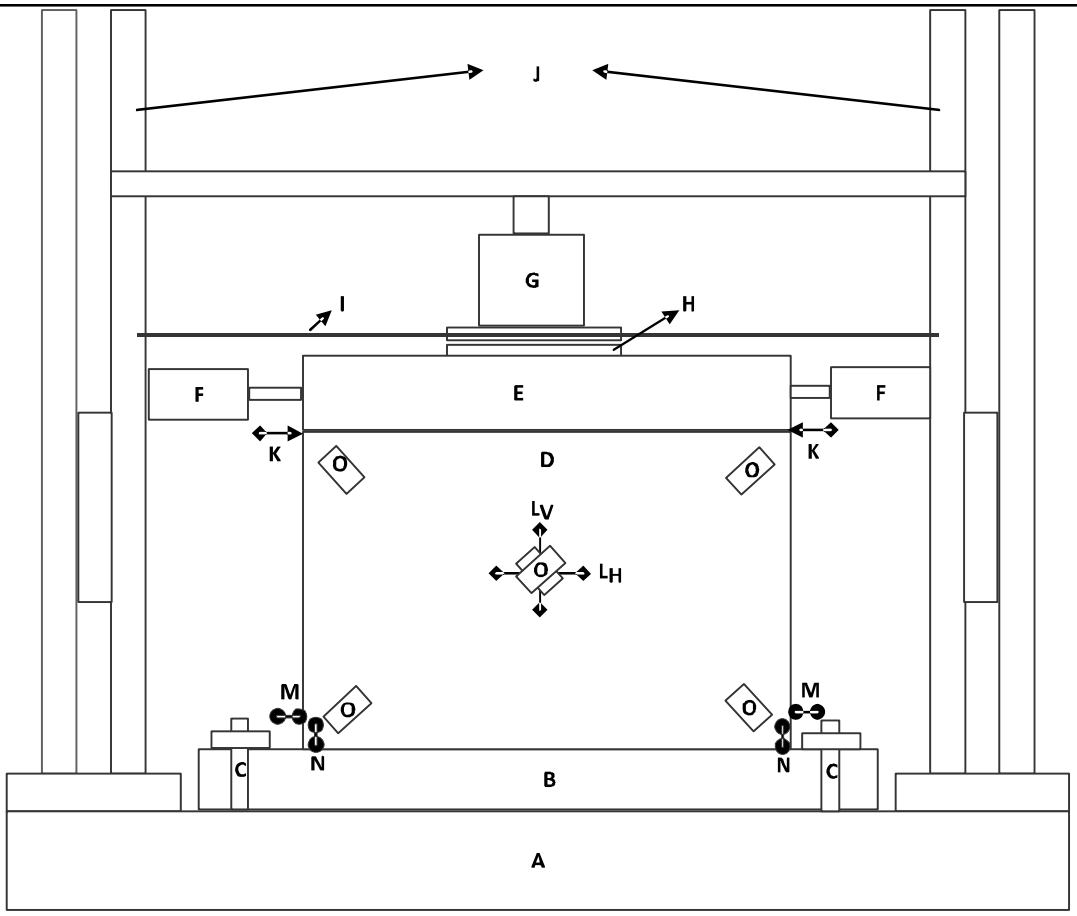

FIG. 3 INSTRUMENTATION OF MASONRY WALL PANEL

LEGENC:

A Strong Floor
B R.C.C. Foundation Beam
C Anchoring Bolts
D Masonry Wall Panel
E R.C.C. Cap Beam
F Lateral Load Jack and Load Cell
G Vertical Load Jack and Load Cell
H Bridge Bearing Assembly
I Horizontal Reaction Anchor Bolts
J Strong Frame
K LVDT at top
L Vertical and Horizontal LDT at strain mode
M LVDT at bottom
N LVDT for up-down
O Strain Gauge

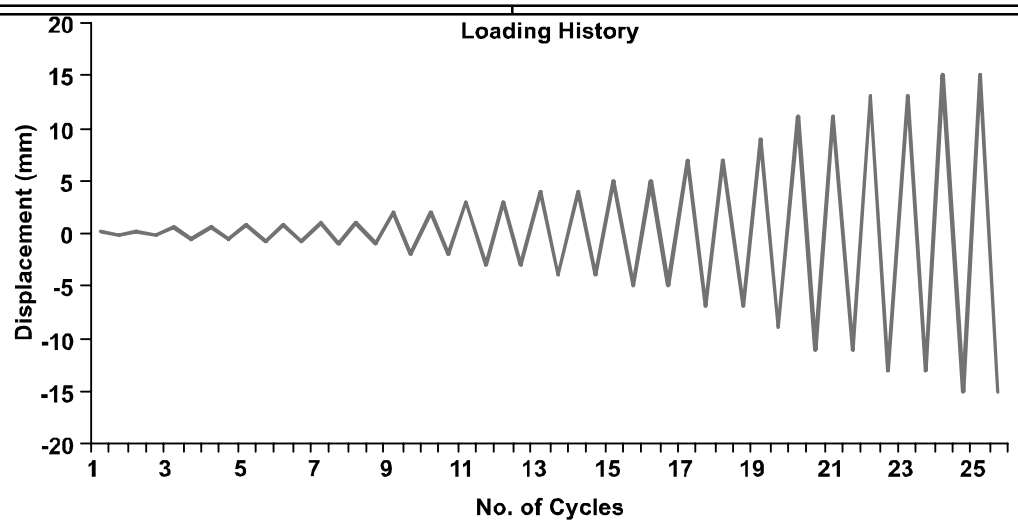

FIG. 4. LOADING HISTORY

6. EXPERIMENTAL TEST RESULTS

The experimental data was recorded and analysed to study the seismic behaviour of un-reinforced walls at different levels of pre-compressions as under:

6.1 WALL 8-URM at 0.5MPa

The Wall 8 was un-reinforced reference specimen tested at 0.5Mpa pre-compression. The peak lateral load was 88.9kN and ultimate displacement at 80% degradation was 3.31mm. The wall exhibited diagonal shear failure and first flexure crack appeared in 9th cycle at middle of the wall at positive direction. The crack was extended from middle of wall to bottom on positive side. On further cycling the cracks propagated on negative and positive directions. The lateral force at yield was 78kN and displacement was 1.63mm. Very less drift ratio was recorded at yield and ultimate stage, which was in the order of 0.15 and 0.3%. The ultimate stage occurred soon after yielding that is the lateral load was 71kN at an ultimate displacement of 3.31mm. At failure the diagonal cracks in both the direction were observed as shown in Fig. 5(a-b).

6.2 WALL 6-URM at 0MPa

The wall 6 was un-reinforced tested at zero pre-compression. The peak lateral load of 14.15kN with 6.4mm ultimate displacement was recorded. The wall exhibited rocking failure and started to rock between last and 2nd last coarse at very early stages of loading that is during 2nd cycle. No cracking or toe crushing was observed during cyclic test due to zero pre-compression. The lateral force and displacement at yield and peak was almost same. At peak stage very less drift ratio of 0.09% was recorded which increased to 0.58% at ultimate stage. The lateral load and displacement at ultimate stage was 11.3kN. The wall experienced rocking failure mode as shown in Fig. 6(a-b).

6.3 WALL 9-URM at 1Mpa

The wall 9 was tested at 1MPa. The peak load recorded was 170.5kN with ultimate displacement of 8.6mm. The wall experienced brittle shear failure due to heavy pre-compression cracks mostly passed through the bricks. The first crack appeared in second last coarse towards positive direction during 9th cycle. Later new cracks passing through bricks appeared at middle top and towards negative direction. Yielding force and displacement was 155kN and 2.1mm. Slight sliding and rocking was also observed at later stages as shown in Fig. 7(a-c) causing higher ultimate displacement. On further cycling, some cracking at wall bottom on both directions were observed

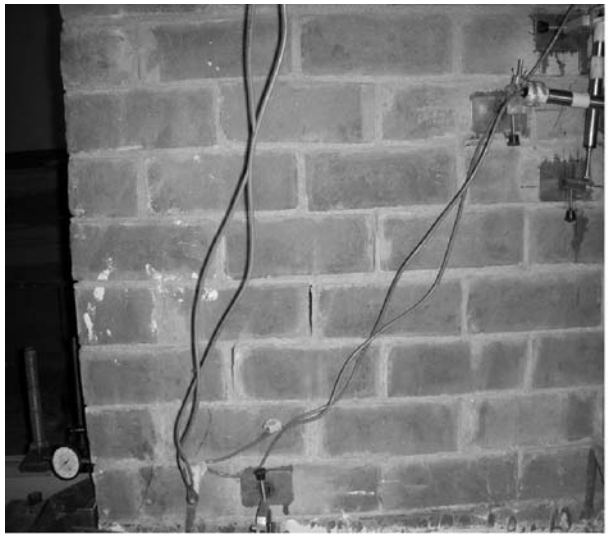

(a)

(b)

FIG. 5. WALL 8 AT FAILURE (A) DIAGONAL CRACKS AT NEGATIVE SIDE (B) DIAGONAL CRACKS AT CENTER TOP

with widening of existing cracks. Very few cracks passed through the mortar. At ultimate that is 80% degradation, the test was stopped and the lateral load was 137kN.

7. DISCUSSION ON TEST RESULTS

The lateral cyclic behavior of the masonry walls with varying levels of pre-compression is discussed in detail in succeeding paragraphs. The different characteristics discussed are lateral force-deformation behavior, hysteretic behavior, energy dissipation, ductility factor, response factor, damping factor, stiffness degradation and behavior of wall at failure.

7.1 Lateral Force-Displacement Behavior

The comparison of lateral strength of reinforced walls with un-reinforced wall is given in Table 2. The lateral load is

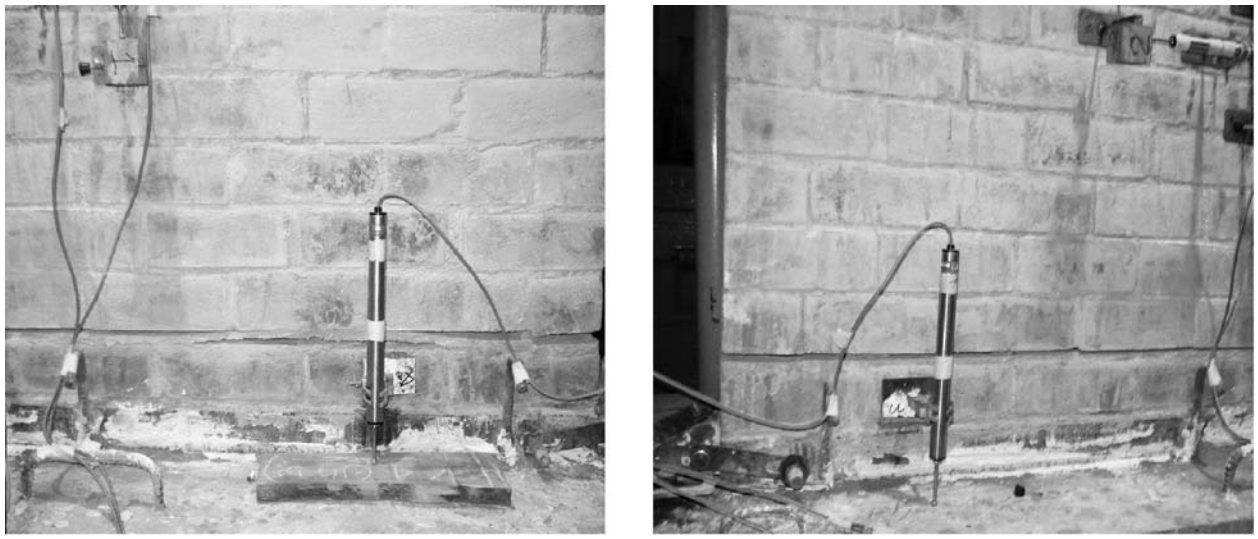

(a) (b)

FIG. 6. WALL 6 AT FAILURE (A) BASE UPLIFT AT POSITIVE SIDE (B) BASE UPLIFT AT POSITIVE SIDE

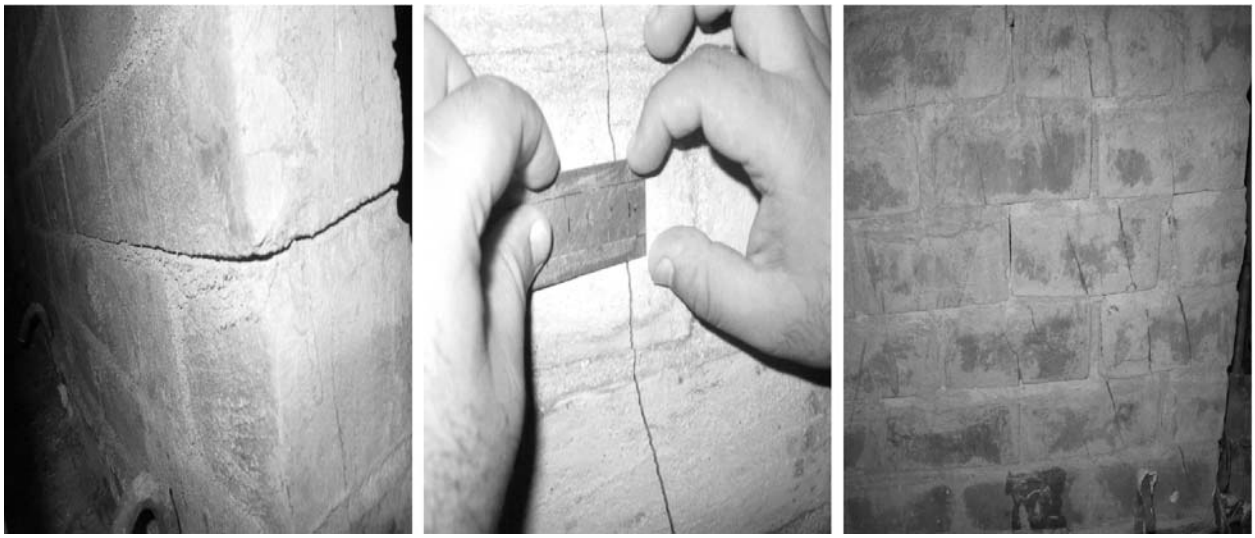

(a) (b) (c)

FIG. 7. WALL 9 AT FAILURE (A) UPLIFT AT POSITIVE SIDE (B) CRACKS PASSING THROUGH BRICKS (C) CRACKING AT TOE

normalized in order to remove variation in the masonry strength from one wall to another. The equation 1 is used to normalize the lateral load. In this equation gross cross-sectional area being constant is not taken into account for all the specimens. The factor 0.22 fm0.5 is used to cater for variation of masonry strength. The factor for reference wall was calculated and ratio for other two walls was found out in comparison to reference wall.

$$\text{Normalized Lateral Load} = \frac{\text{Lateral Load}}{0.22 f_m^{0.5} A_g} \text{x} 100^3 \quad (1)$$

where A_g is Gross cross-sectional area, and f_m is Compressive strength.

Fig. 8 shows the backbone curve of all the walls in both the directions and Fig. 9 shows the critical backbone curves. It is very clear that Wall 9 as expected showed very steep rise in strength and then sudden reduction in strength at the end. Wall 9 with 1Mpa pre-compression has showed maximum strength increase of 92% as expected and least lateral strength is observed in case of Wall 6, which is just 16% of the reference wall 8. The ultimate lateral displacement of URM wall was just 3.31mm and lateral displacement for Wall 9 and Wall 6 were increased by a factor of 2.6 and 1.93 respectively as shown in Figs. 10-11. For Wall 9 the lateral displacement at yield and peak was 1.39 and 2.43 times higher than the reference specimen whereas, the lateral displacement was just 0.6 and 0.35 times of reference wall displacement in case of Wall 6. The yielding and peak lateral force and displacement of Wall 6 was almost same. The higher value of lateral resistance for Wall 9 is primarily due to high pre-compression and higher displacement is due to extensive cracking of bricks.

TABLE 2. SUMMARY OF TEST RESULTS

Parameters	Wall Specimens		
	Wall 8(Reference)	Wall 9	Wall 6
Lateral Load at Yield (kN)	78	155	14.1
Increase wrt URM	1	1.99	0.14
Peak Lateral Load (kN)	88.9	170.5	14.15
Increase wrt URM	1	1.93	0.16
Ultimate Displacement (mm)	3.31	8.6	6.4
Increase wrt URM	1	2.6	1.93
Displacement at Peak (mm)	2.89	7.03	1.0
Increase wrt URM	1	2.43	0.35
Displacement at Yield (mm)	1.63	2.1	0.97
Increase wrt URM	1	1.39	0.6
Ductility	2.03	4.1	6.6
Increase wrt URM	1	2.02	3.25
Cumulative Energy Dissipation (kJ)	1.496	0.94	13.3
Maximum Energy Dissipation Per Cycle (kJ)	0.459	0.125	2.13
Damping Factor (%)	31.8	25	24.7
Maximum Lateral Wall Drift (mm)	1.983	5.23	0.9424
Response Factor (%)	1.75	2.68	3.49
Stiffness Degradation Ratio at Yield (%)	64.28	32.93	100
Stiffness Degradation Ratio at Peak (%)	44.93	21.69	12.51
Maximum Uplift at Wall Base	0.35	2.307	12.1

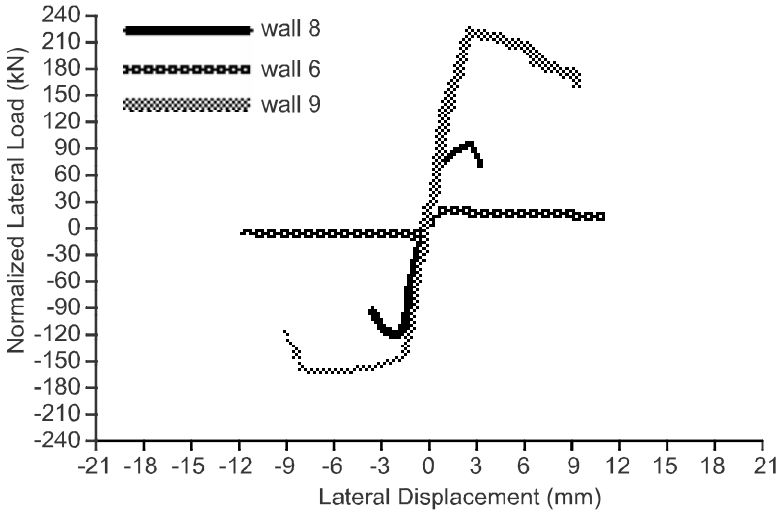

FIG. 8. BACKBONE CURVE ON BOTH SIDES

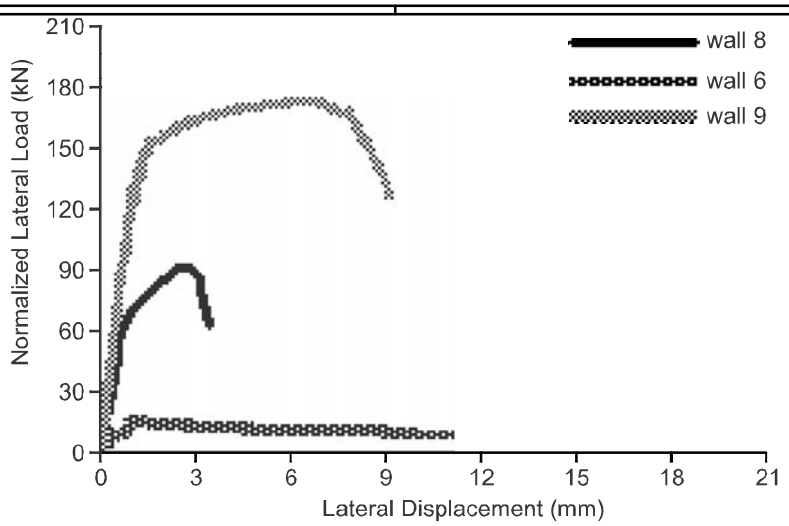

FIG. 9. CRITICAL BACKBONE CURVE

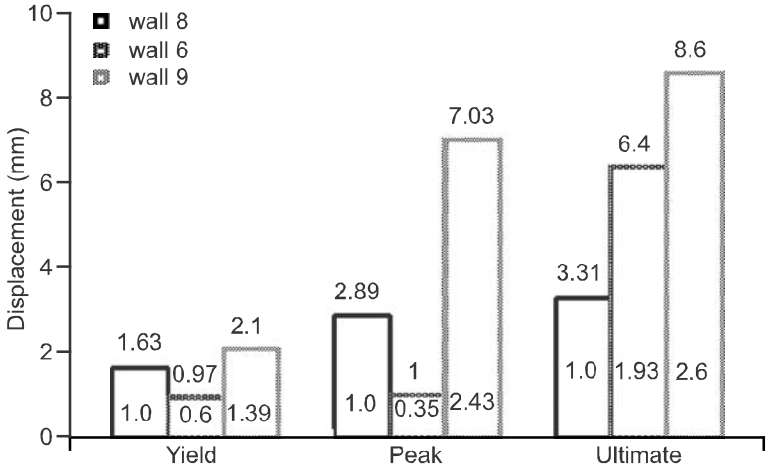

FIG. 10. COMPARISON OF LATERAL DISPLACEMENT AT DIFFERENT STAGES

Due to some rocking and sliding after the yielding, the wall has maintained the force in in-elastic region after which there is sudden fall in strength due to cracking in the toe/heel region. After yielding at 2.1mm the peak stage has been delayed till 7.03mm due to rocking mode of failure. The higher pre-compression facilitated higher strength initially and then rocking/sliding delayed the sudden degradation of wall. Wall 6 showed very less strength gain due to absence of pre-compression. At earlier stages the wall started rocking and the increase in strength was seized and yielding stage occurred very soon. It maintained the strength after yielding for higher displacement and strength degradation was very slow. Wall 8 also showed sudden strength increase followed by sudden reduction in strength due to heavy cracking. Very less drift ratio of 0.097% was achieved for Wall 6 at yielding stage as shown in Fig. 12. However, at ultimate stage, the drift ratio increased to 1.9 and 2.6 times as compared to reference wall.

7.2 Hysteretic Behavior

The hysteretic behavior of all the three walls is shown in Figs. 13-15. The nonlinear elastic response of Wall 8 is quite evident but the inelastic response is very poor due to sudden fall in strength. The wall reached its peak load and than there is a sudden drop in lateral strength showing typical brittle behavior. The narrow hysteretic loop is due to lower residual displacement prior to cracking whereas, it get quite high after initiation of cracking. Uptill elastic

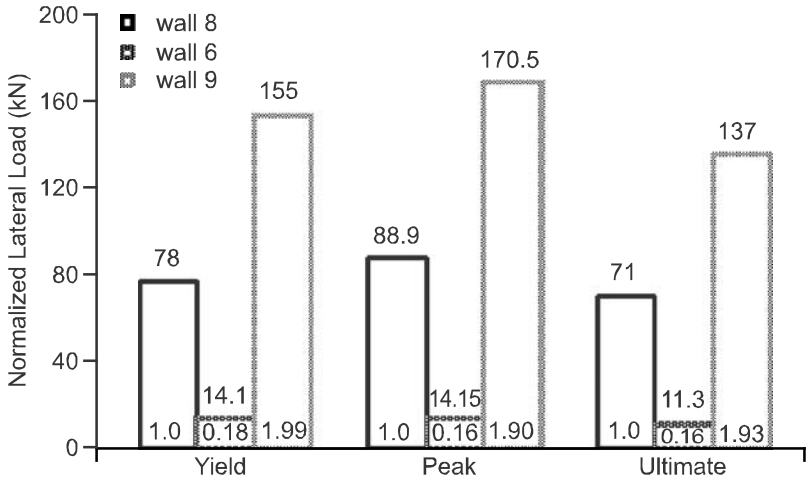

FIG. 11. COMPARISON OF NORMALIZED LATERAL STRENGTH AT DIFFERENT STAGES

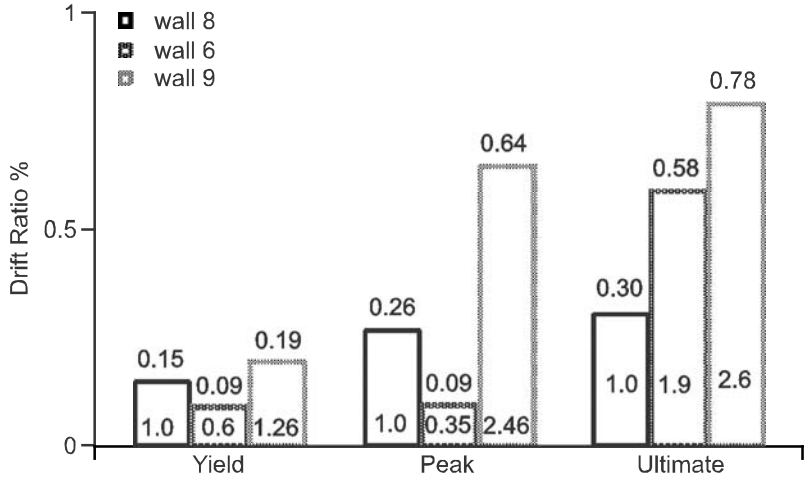

FIG. 12. COMPARISON OF DRIFT RATIO AT DIFFERENT STAGES

stage the behaviour of Wall-9 is quite similar to reference wall with higher lateral strength but after yielding, the hysteretic loops are quite widened due to slight rocking/ sliding. After the peak the wall experienced sudden drop in strength, a typical characteristic of URM wall. The residual displacement was also higher.

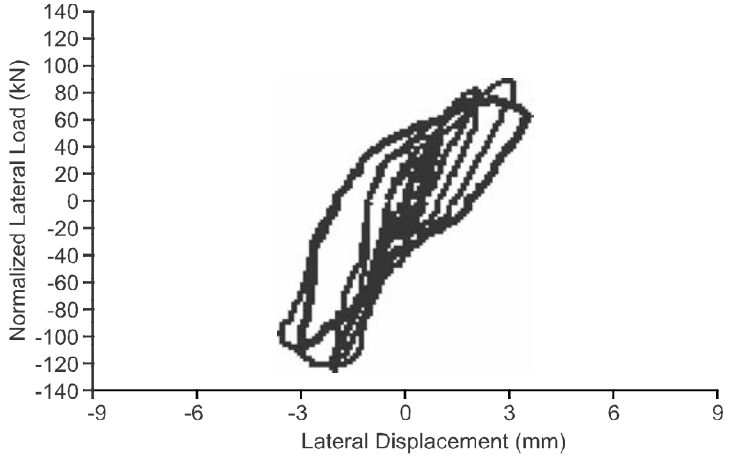

FIG. 13. HYSTERETIC RESPONSE OF WALL 8

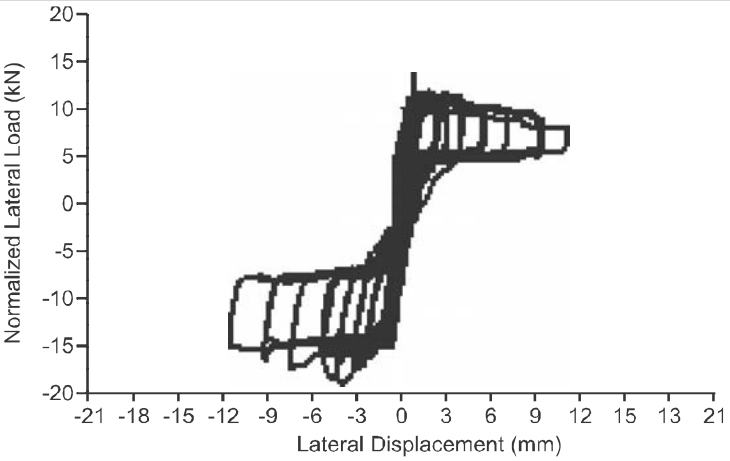

FIG. 14. HYSTERETIC RESPONSE OF WALL 6

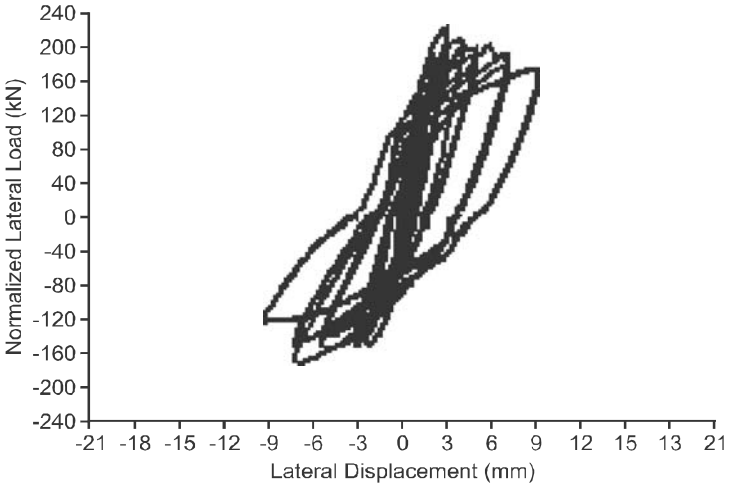

FIG. 15. HYSTERETIC RESPONSE OF WALL 9

The hysteretic loop of Wall 6 is quite interesting. Yielding and peak stage occurred at the end due to excessive rocking. The peak load lateral load achieved was quite low due to start of rocking at very early stages of cycling. After start of rocking the wall maintained the force and dissipated the energy through displacement increase. The loop is fanned out at the top but narrowing at bottom. However, the width of hysteretic loops for all the three walls was narrow with less energy dissipation, a peculiar characteristic of URM wall. The residual displacement after each cycle is shown in Fig. 16.

7.3 Energy Dissipation

High-energy dissipation is a desirable property when a structure is subjected to a severe seismic event. The area enclosed by the hysteretic loop represents the energy dissipated by the specimen. The cumulative energy dissipation of the specimens can be calculated by adding energy consumed during each loading cycle.

Figs. 17-18 show the energy dissipated during each cycle and cumulative energy absorbed in all the cycles. The energy dissipated during cyclic loading mainly depends upon the friction along joints; widening/new cracks formation, crushing of bricks; rocking and toe crushing. The failure mode also affects the amount of energy dissipated. If the wall experience rocking or sliding failure then energy dissipated will be less despite of higher lateral strength as rocking failure is characterized by the property of specimen to come back to its origin. Whereas, in case of cracking the residual displacement will be more and despite of less lateral force energy dissipated will be more. The Wall 8 experienced cracking failure but its energy dissipation was less due to sudden drop in lateral strength and absence of inelastic branch. The wall dissipated maximum of 0.459kJ energy in one cycle and its cumulative energy dissipated during all the cycles was just 1.496kJ.

The energy dissipated per cycle by Wall 6 was much less than reference wall due to sudden start of rocking and lower lateral strength. 0.125kJ was the dissipated energy per cycle and cumulative energy for Wall was 0.94kJ. Wall 9 experienced higher energy dissipation of 2.13kJ per cycle and its cumulative energy dissipated was 13.3kJ, which was much higher than the reference wall. The higher energy dissipated is attributed to higher lateral strength, higher residual displacement and the wall also sustained the stiffness during inelastic branch and peak stage occurred later. Table 2 summarizes test results obtained for all the specimens.

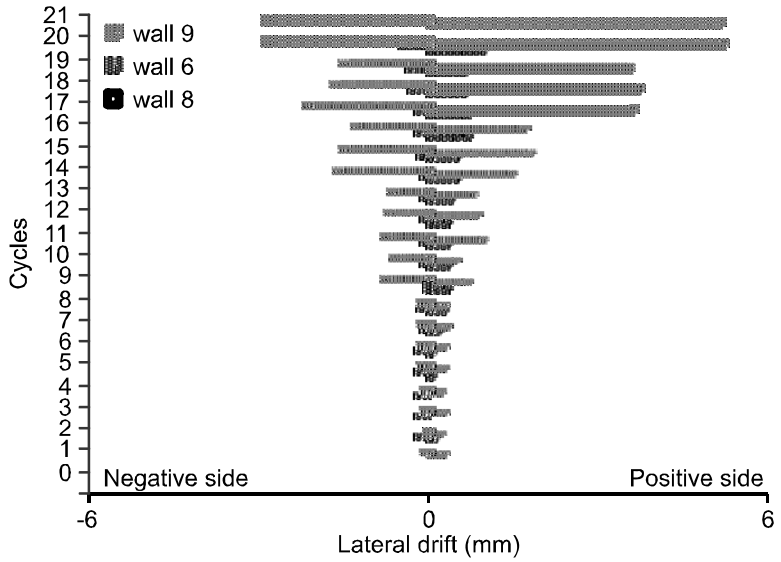

FIG. 16. COMPARISON OF RESIDUAL DISPLACEMENT/CYCLE

7.4 Dictility and Response Factor

Ductility is the most important factor of performance of any structural system in the seismic prone area. The displacements at yielding, peak and ultimate stages were calculated by using a method proposed by Mugruma [21]. Using these displacement values the displacement ductility was calculated for all the specimens. Ductility of the test specimens is compared in Fig. 19. The failure mode also affects the ductility. In rocking failure the specimen tends to return to its origin and the peak stage is delayed. Higher ductility factor in order of 3.25 and 2.02 times were recorded in case of Wall 6 and 9 respectively. The higher ductility factor in case of Wall 9 was due to extended inelastic branch as the wall went into rocking and sliding after yielding. In case of Wall 6 higher ductility factor is attributed because the yielding occurred very soon at just 0.97mm of displacement and ultimate displacement was 6.4mm.

Response factor is an important factor in seismic designing of any structure behavior of shear walls. The response factor of the specimens is determined by using the Equation (2) provided by Paulay and Priestley [16].

$$R_f = \sqrt{\left(2\mu_d - 1\right)} \tag{2}$$

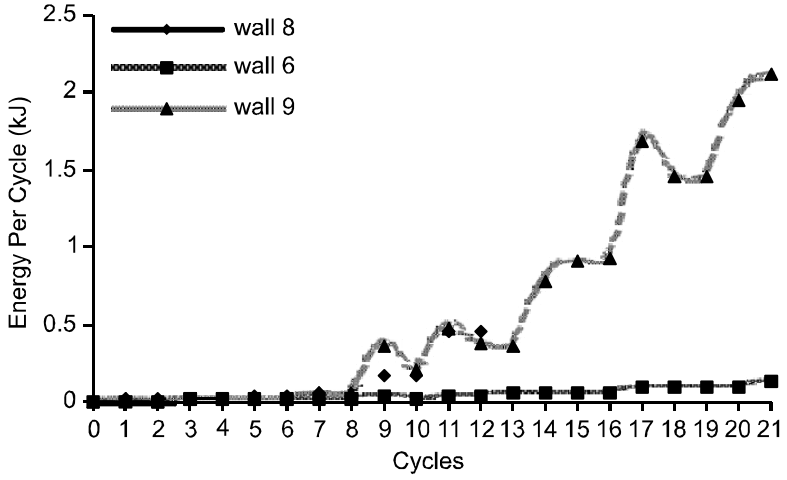

FIG. 17. COMPARISON OF ENERGY ABSORBED PER CYCLE

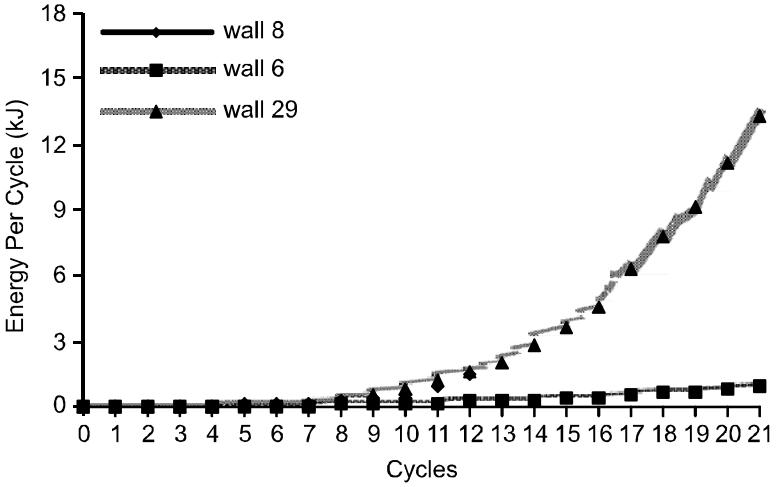

FIG. 18. CUMULATIVE ENERGY DISSIPATION IN ALL CYCLES

Where μ_d is the ductility factor. Higher value of response factor was achieved in case of Wall 6 due to higher ductility factor. An increase in response factor of 99 and 53% was calculated for Wall 6 and Wall 9 respectively as shown in Fig. 20.

7.5 Damping Factor

An approximate value of the equivalent viscous damping of the specimens, was also obtained by using equation 3 which was used by Elgawady [22]:

$$\zeta = 1/2\pi(A_1/A_2) \quad (3)$$

where A_1 is energy dissipated in a cycle i.e. area inside the loop and A_2 is strain energy measured at the peak force of the same cycle (sum of hatched area), i.e. the sum of the hatched areas under the triangles. Fig. 21 shows the method to calculate the equivalent viscous damping of all the three specimens as a function of lateral displacement. A damping value of 7-10% is quite reasonable for design of un-reinforced masonry. The damping factor value for reference wall was quite high that is 32% due to severe diagonal cracking. Elgawady [22] has also quoted 30% damping factor for URM wall as shown in Fig. 22. The maximum damping values of 25 and 24.7% were recorded for Wall 6 and 9 respectively. Less values for both the walls were primarily due to rocking mode of failure.

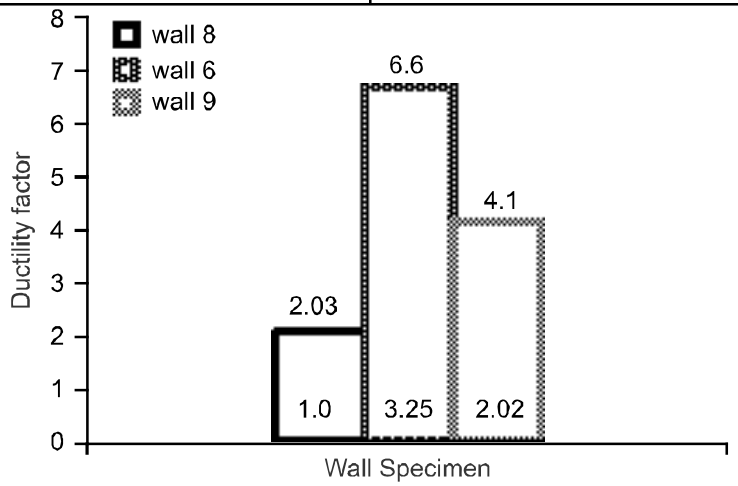

FIG. 19. DUCTILITY FACTOR FOR ALL SPECIMENS

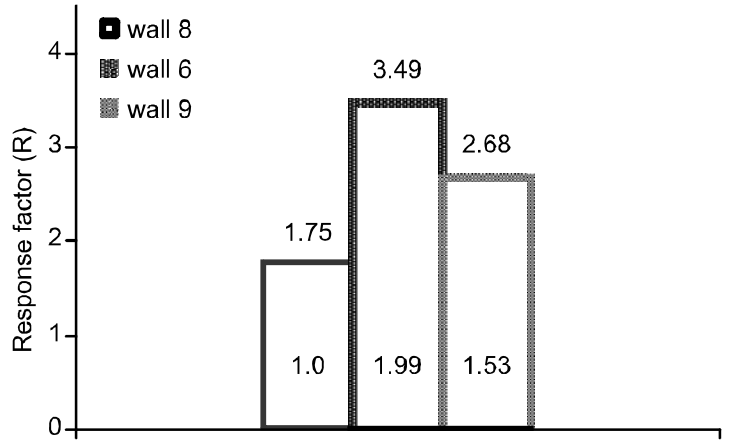

FIG 20. RESPONSE FACTOR FOR ALL SPECIMENS

7.6 Stiffness Degradation

The equivalent elastic-perfectly plastic model proposed by Mugruma [21] was used to determine yield, peak and ultimate load stages from the load-displacement curve. Stiffness degradation ratio (C_k) is the rate of stiffness reduction beyond yield. The ratio of secant modulus at specified displacement (K) to the secant modulus at yield (K_o) is shown in Equation (4).

$$C_k = K/K_o \quad (4)$$

Where K_o is the slope of line passing through origin and yield point. Stiffness degradation ratios at peak (K_p) and at ultimate stage (K_u) were calculated by determining the slopes of lines passing through peak and ultimate point. C_k at peak and ultimate was calculated and plotted in Fig. 23. In case of Wall 6 the stiffness degradation was 100 and 33% for wall 9. At ultimate stage the stiffness degradation of Wall 6 and 9 was quite less than the reference wall.

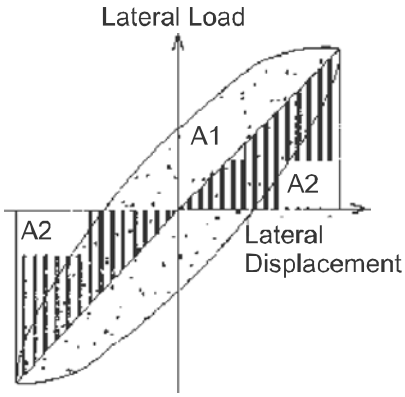

FIG. 21. METHOD FOR DAMPING FACTOR CALCULATION

Stiffness degradation trend for all the three walls is shown in Fig. 24. A sudden downward stiffness degradation trend for reference wall was recorded due to its brittle behavior. Wall 9 also showed sudden fall after the peak but later some recovery is visible due to start of rocking.

Wall-6 showed very mild downward trend due to start of rocking at initial stages.

7.7 Behavior Wall at Failure

The lateral drift and uplift of wall are the important parameters for describing the failure mode of the wall. Figs. 25-26 show the maximum lateral drift and base uplift of wall during the cyclic test. As the Wall 6 experienced rocking failure its base uplift was maximum that is upto 12mm and lateral drift was minimum 0.94mm with peculiar characteristics of rocking mode of failure. 2.31mm and 5.23mm was the recorded values of base uplift and lateral drift of Wall 9 as the wall experienced cracking with some rocking after yielding. Reference wall experienced diagonal failure with no rocking and recorded values of wall lateral drift and base uplift were 1.983 and 0.35mm respectively, which is a peculiar characteristic of diagonal shear failure.

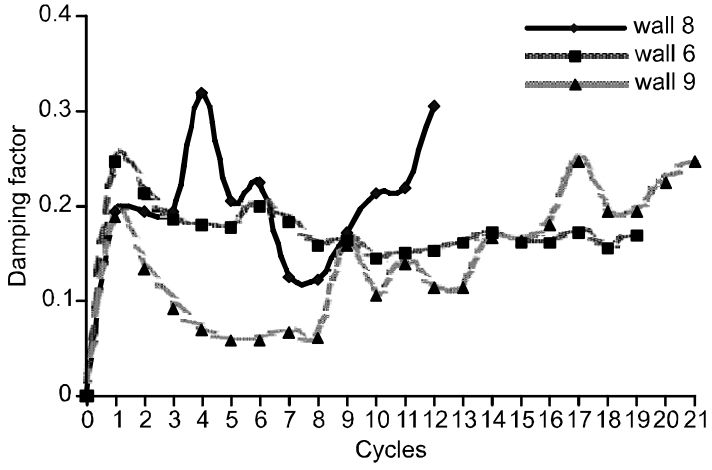

FIG. 22. DAMPING FACTOR FOR ALL SPECIMENS

8. CONCLUSIONS

The static cyclic tests were conducted on un-reinforced masonry wall panels to compare the effect of pre-compression on seismic performance of masonry under cyclic loading. It was found that the level of pre-compression plays an important role on lateral resistance, displacement, ductility and energy dissipation. The conclusions and observations made after the tests are as follows:

(i) By doubling the pre-compression the lateral strength has increased by a factor of 1.93 times and at zero pre-compression the lateral strength was just 16% of reference wall. The lateral displacement at ultimate stage was 2.6 and 1.93 times more than that of reference wall. The increase in lateral displacement is primarily due to rocking mode of failure.

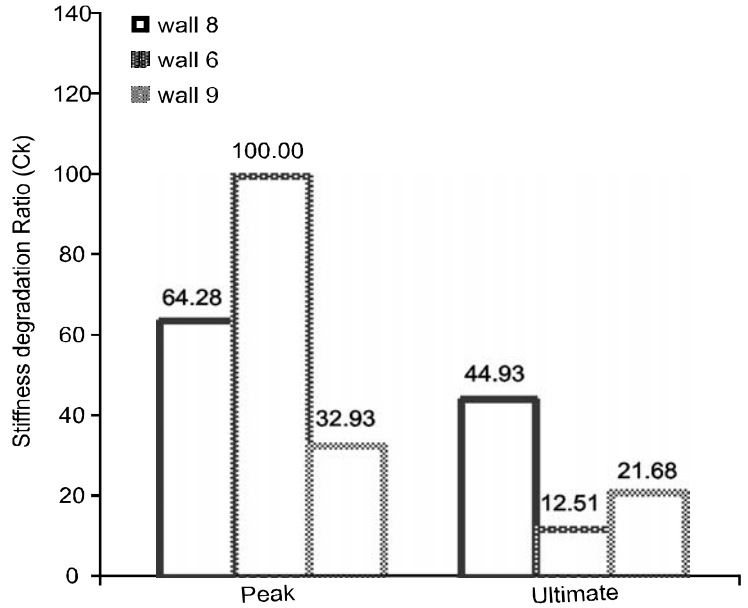

FIG. 23. COMPARISON OF STIFFNESS DEGRADATION RATIO

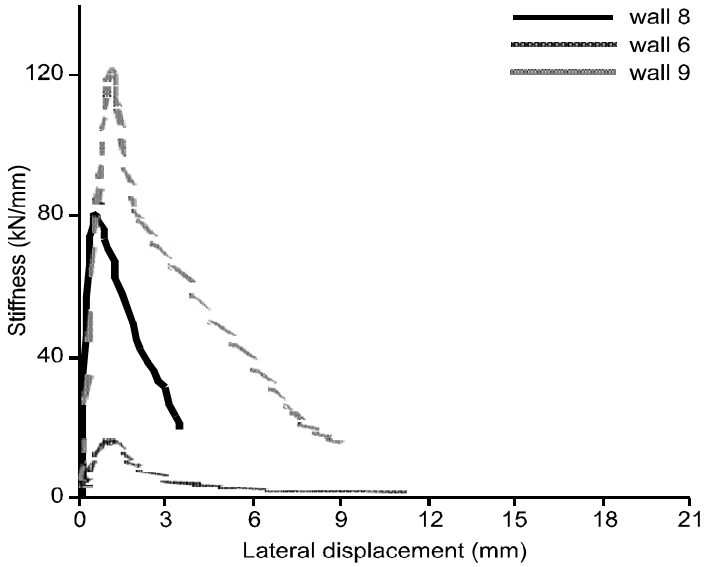

FIG. 24. COMPARISON OF STIFFNESS DEGRADATION TREND

(ii) The energy dissipated by URM wall tested at 1.0Mpa pre-compression was 8.9 times higher than reference wall as it experienced cracking at toe, cracking of bricks, rocking after yielding causing slightly prolonged inelastic branch and delayed peak stage. Energy dissipated by URM wall tested at 0.0Mpa pre-compression was very less than the reference wall due to lower lateral strength.

(iii) The displacement ductility of URM wall tested at 0.0Mpa pre-compression and in case of URM wall tested at 1Mpa pre-compression it was 3.25 and 2.02 times more than that of reference wall respectively. It is observed that strengthened masonry walls showed very good ductility as compared to URM. The response factor improved by a factor of 99 and 53% for Wall 6 and Wall 9.

(iv) A higher value of 32% as damping factor was recorded for URM wall due to severe cracking and lesser values of about 25% were recorded for other two walls as both of them went into rocking.

(v) The failure mode also plays an important role in seismic behavior of masonry and it depends upon the boundary condition, level of pre-compression and shear strength of masonry. By controlling the failure mode, the desired behaviour can be achieved.

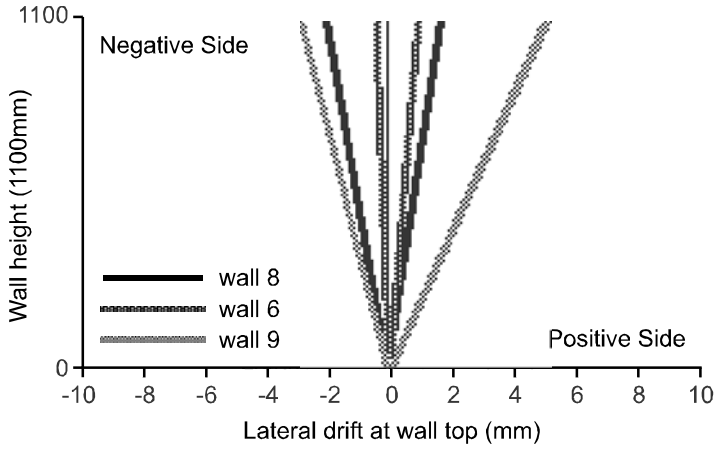

FIG. 25. LATERAL DRIFT OF WALL SPECIMENS

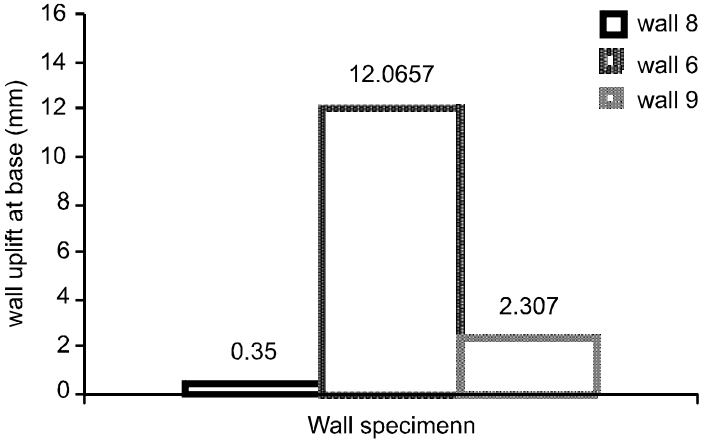

FIG. 26. MAXIMUM BASE UPLIFT

ACKNOWLEDGEMENTS

The authors would like to thank Higher Education Commission, Islamabad, and University of Engineering & Technology, Lahore, Pakistan, and Dr. Wajahat Mirza, SIKA (Pvt.) Limited, for providing assistance to complete this research work.

REFERENCES

[1] Ilyas, M., and Farooq, S.H., "Collapse of a Building Due to Percolation of Water from Rooftop in Old Lahore", Proceeding of 7th International Summer Symposium, Tokyo, Japan, 41-44, 2005.

[2] Farooq, S.H., and Ilyas, M., "A Study on Failure Pattern Observed in Masonry Building During 8th October, 2005 Earthquake in Pakistan", Proceeding of 7th International Conference on Civil Engineering, Tehran, Iran, May 8-10, 2006.

[3] Ashraf, M., Ilyas, M., and Farooq, S. H., "A Case Study: Hazara University Affected by Recent Earthquake", Proceeding of International Conference on Earthquake Engineering, Lahore, Pakistan, September 8-9, 2006.

[4] Ilyas, M., Rizwan, M., and Farooq, S. H., "Ground Failure and Structural Damages During Recent Earthquakes in Northern Areas of Pakistan", Proceeding of First National Seminar on Geotechnical Aspects of Hydropower Projects, pp. 149-160, Pakistan, 2005.

[5] Farooq, S.H., Ilyas, M., and Ghaffar, A., "Technique of Strengthening Masonry Wall Panels using Steel Strips", Asian Journal of Civil Engineering (Building and Housing), Volume 7, No. 6, pp. 625-642, Iran, 2006.

[6] Farooq, S.H., Ilyas, M., and Ghaffar, A., "Effect of Horizontal Reinforcement in Strengthening of Masonry", Mehran University Research Journal of Engineering & Technology, Volume 27, No. 1, pp. 49-62, Jamshoro, Pakistan, January, 2008

[7] Matsumura, A., "Shear Strength of Reinforced Masonry Walls", Proceedings of 9th World Conference on Earthquake Engineering, Volume 7, pp. 121-126, Tokyo, Japan, 1988.

[8] Shing, P.B., Schuller, M., and Hoskere, V.S., "In-Plane Resistance of Reinforced Masonry Shear Walls", ASCE Journal of Structural Engineering, Volume 116, No. 3, pp. 619-640, 1990.

[9] NZS 4230, "Code of Practice for the Design of Masonry Structures", Standards Association of New Zealand, Wellington, 1990.

[10] Anderson, D.L., and Priestley, M.J.N., "In Plane Shear Strength of Masonry Walls", Proceedings of 6th Canadian Masonry Symposium, pp. 223-234, Saskatoon, Saskatchewan, 1992.

[11] Uniform Building Code, "International Conference of Building Officials", Volume 2, pp. 492, Whittier, California, April 1997.

[12] AS-3700, "Masonry Structures", Standards Association of Australia, Homebush, NSW, Australia, 1998.

[13] Matsumura, A., "Planar Shear Loading Test on Reinforced Fully Grouted Hollow Clay Masonry Walls", Proceedings of 5th North America Masonry Conference, University of Illinois, pp. 347-356, Urbana-Champaign, 1990.

[14] Chen, Shi-Wen J., Hidalgo, P.A., Mayes, R.L., Clough, R.W., and McNiven, H.D., "Cyclic Loading Tests of Masonry Single Piers, Height to Width Ratio of 1", Volume 2, Report No. UCB/EERC-78/28, Earthquake Engineering Research Centre, University of California, Berkeley, CA, 1978.

[15] Sveinsson, B.I., Mayes, R.L., and McNiven, H.D., "Cyclic Loading of Masonry Single Piers", Volume 4, Report No. UCB/EERC-85/15, Earthquake Engineering Research Centre, University of California, Berkeley, 1985.

[16] Woodward, K., and Rankin, F., "Influence of Block and Mortar Strength on Shear Resistance of Concrete Block Masonry Walls", NBSIR 85-3143, National Bureau of Standards, Gaithersburg, MD, 1985.

[17] Woodward, K., and Rankin, F., "Influence of Aspect Ratio on Shear Resistance of Concrete Block Masonry Walls", NBSIR 84-2993, National Bureau of Standards, Gaithersburg, MD, 1985.

[18] Okamoto, S., Yamazaki, Y., Kaminosono, T., Teshigawara, M., and Hirashi, H., "Seismic Capacity of Reinforced Masonry Walls and Beams", Proceedings of 18th Joint Meeting of the US-Japan Cooperative Program in Natural Resource Panel on Wind and Seismic Effects, NBSIR 87-3540, National Institute of Standards and Technology, pp. 307-319, Gaithersburg, 1987.

[19] Kaminosono, T., Teshigowara, M., Hiraishi, H., Fujisawa, M., and Nakaoka, A., "Experimental Study on Seismic Performance of Reinforced Masonry Walls", Proceedings of 9th World Conference on Earthquake Engineering, pp. 109-114, Tokyo-Kyoto, Japan, 1988.

[20] Shing, P.B., Brunner, J.D., and Lotfi, H.R., "Evaluation of Shear Strength of Reinforced Masonry Walls", TMS Journal, Volume 12, No. 1, pp. 65-77, 1993.

[21] Muguruma, H., Nishiyrama, M, Watanabe, F., and Tnaka, H., "Ductile Behavior of High Strength Concrete Columns Confined by High Strength Transverse Steel", ACI Special Publication Evaluation and Rehabilitation of Concrete Structures and Innovation in Design, Volume 128, No. 54, pp. 88, 1991.

[22] ElGawady, M.A., Lestuzzi, P., and Badoux, M., "Static Cyclic Response of Masonry Walls Retrofitted with Fiber Reinforced Polymer", Journal Computer for Construction, ASCE, Volume 10, No. 1, 2007.